JOURNAL OF SPACECRAFT AND ROCKETS
Vol. 32, No. 2, March–April 1995

Missile Aerodynamics at High Angles of Attack: A Prediction Code

S. Venugopal*
Defence Research and Development Laboratory, Hyderabad, India
and
M. Krishnamurthy†
National Aerospace Laboratories, Bangalore, India

A computer code MAHAA has been developed for estimating the aerodynamic characteristics of cruciform missile configurations at high angles of attack (up to 30 deg), with arbitrary control deflections (±25 deg) and nonzero roll angle ($0 \leq \phi \leq 90$ deg). The prediction code is based on the equivalent-angle-of-attack technique. It combines semiempirical methods, theoretical methods, and correlated databases. The code has been validated over a wide range of missile configurations and flight parameters. The overall capabilities of the code have been compared with nine other missile aeroprediction codes. These studies have demonstrated the capability of the code for preliminary design of missile configurations.

Nomenclature

a	= local body radius
AR	= aspect ratio
C	= fin chord
C_l	= rolling-moment coefficient
C_m	= pitching-moment coefficient
C_N	= normal-force coefficient
C_n	= yawing-moment coefficient
C_Y	= side-force coefficient
K_B	= body carryover factor
K_W	= wing–body interference factor
K_ϕ	= interference factor due to roll
k_B	= body carryover factor due to fin deflection
k_w	= wing–body interference factor due to fin deflection
M	= Mach number
s	= semispan of fin alone
s_m	= maximum semispan of fin including the body
t	= fin thickness
α	= angle of attack
α_{eqi}	= equivalent angle of attack of fin i
$\Delta\alpha_{vi}$	= average angle of attack induced on the fin i due to vortices
δ_i	= deflection of fin i
Λ_{ji}	= fin deflection factor
λ	= taper ratio
λ_{ji}	= ratio of the partial area of fin j influenced by fin i to the fin planform area
ϕ_i	= roll angle of fin i

Introduction

PRELIMINARY design of missiles requires rapid engineering methods for the estimation of their aerodynamic characteristics. Quick-reacting, highly maneuvering tactical missile design requires the prediction of these characteristics well into the nonlinear range. The commonly used component buildup method is incapable of predicting the aerodynamic characteristics accurately in this high-angle-of-attack range. The equivalent-angle-of-attack concept, which is a comprehensive extension of the component buildup method, is a powerful technique and can be used for this purpose.[1]

This paper presents the details of a computer code MAHAA developed according to the equivalent-angle-of-attack methodology for computing the aerodynamic characteristics of cruciform body–canard–wing–tail combinations over a wide range of geometric as well as flight parameters. The MAHAA code can estimate five static aerodynamic characteristics of missiles, namely, normal force, side force, pitching moment, yawing moment, and rolling moment. The methodology combines semiempirical methods, analytical methods, and correlated databases on the basis of analysis and engineering assumptions. A vast number of correlated experimental databases, especially for wing-alone characteristics, centers of pressure, and wing–body interference, have been used. Further, a vortex tracking method that is appropriate for a situation when the vortices are asymmetric in strength and disposition has been developed and implemented to cater for nonzero roll orientations and arbitrary control deflections. This, along with improved experimental data inputs and correlations, has led to better utilization of the potentials of the equivalent-angle-of-attack concept and resulted in better predictions.

MAHAA has been validated against available experimental data over a wide range of configurations in the high-angle-of-attack and-Mach-number regimes. Also, its prediction capabilities have been compared with nine other aeroprediction codes. These validation studies have established it as a state-of-the-art code. The program is written in Fortran 77 in a modular fashion so that future modifications can be incorporated easily as and when more data bases and better methods become available. A typical run time on the VAX 11/785 machine is 2 CPU seconds per data run for a wing–body–tail configuration.

The range of applicability of the code is directly related to the range of the databases used and is summarized below:

Angle of attack	$-30 \leq \alpha \leq 30$ deg
Mach number	$0.8 \leq M \leq 5.0$
Roll angle	$0 \leq \phi \leq 90$ deg
Control deflection	$-25 \leq \delta \leq 25$ deg
Fin aspect ratio	$0.5 \leq \text{AR} \leq 4.0$
Fin taper ratio	$0 \leq \lambda \leq 1.0$
Body nose fineness ratio	0.5 to 8.0
Afterbody fineness ratio	0 to 20.0

The MAHAA code is applicable to an axisymmetric body in combinations with canard, wing, and tail. The code considers sector, hemispherical, pointed or blunt conical, or ogival nose shapes and a cylindrical afterbody. The effect of flares and boattail are not

Received Nov. 30, 1992; revision received March 31, 1993; accepted for publication April 2, 1993. Copyright © 1995 by the American Institute of Aeronautics and Astronautics, Inc. All rights reserved.

*Scientist, Aerodynamics Division.
†Scientist, Experimental Aerodynamics Division.

included. The lifting and control surfaces should have zero or small trailing-edge sweep angles. The airfoil section is assumed to be thin ($t/C < 0.06$), and the details of the airfoil geometry are not considered.

Methodology

The total normal-force and pitching-moment coefficients of a wing–body–tail configuration can be written as the sums of individual component contributions according to the component buildup method as

$$C_{N\,BWT} = C_{N\,B} + C_{N\,W(B)} + C_{N\,B(W)} + C_{N\,T(B)} + C_{N\,B(T)} + C_{N\,T(W)} \tag{1}$$

$$C_{M\,BWT} = C_{M\,B} + C_{M\,W(B)} + C_{M\,B(W)} + C_{M\,T(B)} + C_{M\,B(T)} + C_{M\,T(W)} \tag{2}$$

The subscripts are defined as follows:

BWT = complete wing–body–tail configuration
B = body alone
$W(B)$ = wing in the presence of the body
$B(W)$ = increment for the body in the presence of the wing
$T(B)$ = tail in the presence of the body
$B(T)$ = increment for the body in the presence of the tail
$T(W)$ = tail in the presence of the wing

In the linear range for moderate supersonic speeds and small angles of attack, the terms in Eqs. (1) and (2) arise from a linear superposition of the flowfields.[1] To allow for the nonlinearities arising at high angles of attack, the equivalent-angle-of-attack concept is adopted. The crux of this method lies in considering the wing and tail panel loads separately from those acting on the body and replacing the linear dependence of these loads on the angle of attack by nonlinear functional relationships. Further, each contribution to the normal force of the missile is considered in terms of an equivalent increment in the fin-alone angle of attack, and these incremental angles of attack are added to get the total equivalent angle of attack (α_{eq}) of the fin. In the higher α range, the nonlinearity is further included by linearly adding the velocity components rather than the angles of attack.[1] Thus for the ith fin, the equivalent angle of attack is given as[2]

$$\tan\hat{\alpha}_{eqi} = K_W \tan\alpha\cos\phi_i + \frac{4}{\text{AR}} K_\phi \tan\alpha\sin\alpha\sin\phi_i\cos\phi_i + \tan\Delta\alpha_{vi} \tag{3}$$

$$\tan\alpha_{eqi} = \tan\hat{\alpha}_{eqi} + \sum_{j=1}^{4}\tan(\Lambda_{ji}\delta_j) \tag{4}$$

where K_W, K_ϕ, and Λ_{ji} are interference factors and $\hat{\alpha}_{eqi}$ is the equivalent angle of attack for no fin deflection. The normal-force coefficient of the interactioned fin can be obtained from the equivalent angle of attack by using the wing-alone normal-force characteristics. The contribution to the moments from lifting fins are obtained by estimating the centers of pressure of these forces on individual fins. The complete aerodynamic characteristics are finally estimated by adding the body-alone and the body carryover terms.

The interference factors appearing in Eqs. (3) and (4) are functions of angle of attack and Mach number, and suitable choice of these parameters is vital for an accurate estimation of the equivalent angle of attack.

Wing–Body Interference Factor K_W

The wing in the presence of a body at an angle of attack experiences an increase in wing lift due to body upwash. K_W is a measure of this interference effect, and its value is generally greater than unity, implying favorable interference. This favorable lift can decrease or even be reversed at higher angles of attack and speeds. This is due to large regions of flow separation or deflection of flow parallel to the surface, resulting in loss of upwash and dynamic pressure.

In the absence of any theoretical method to account for these effects, K_W is estimated using a correlated experimental data base in the present study. This method makes use of the limited experimental data base for K_W available in Ref. 3. The data have been correlated with the parameter $|1 - M^2\sin^2\alpha|$, which includes the freestream Mach number as well as the angle of attack. The details of the method are presented in Ref. 4, and K_W is predicted within ±10% accuracy.

Interference Factor Due to Roll, K_ϕ

The interference factor K_ϕ takes account of the change in normal force due to the effect of roll angle. The change in normal force arising from roll will be different for windward and leeward positioning of fins. In the absence of any experimental data on K_ϕ for higher angles of attack and Mach numbers, it is computed on the basis of slender-body theory (SBT).[5]

Fin Deflection Factor Λ_{ji}

If a fin of a cruciform wing–body combination is deflected arbitrarily, the flowfield induced by this deflection develops a primary normal force on the deflected fin (direct effect) and induces secondary normal forces on the other three, undeflected fins (called fin–fin interference). SBT defines a fin deflection factor (also called control effectiveness parameter) Λ_{ji}, which allows for these effects. According to SBT, Λ_{ji} is dependent only on the ratio a/s_m; it is assumed that the fins are entirely within each others' region of influence. However, this is not the case at supersonic speeds, where the fins may be partially within the region of influence of each other at any finned section.[1] As an engineering analysis based on linear theory, this effect is taken into account by reducing Λ_{ji} by a factor λ_{ji}, which is defined as the ratio of the partial area of influence of the fin (S_{ji}) to the fin planform area (S_F). The code estimates λ_{ji} from the zero-angle-of-attack case given in Ref. 3. The incremental angle of attack for the ith fin due to fin deflections can be written as

$$(\tan\Delta\alpha_{eqi})_\delta = k_w\{\tan(\hat{\alpha}_{eqi} + \delta_i) - \tan\hat{\alpha}_{eqi}\} + k_w\sum_{\substack{j=1\\ j\neq i}}^{4}\lambda_{ji}\tan(\delta_j\Lambda_{ji})$$

where k_w is the interference factor due to deflection.

Wing–Body Interference Due to Wing Deflection, k_w

The factor k_w is a measure of the interference of the body on the wing due to its deflection. According to SBT, k_w is a function of a/s_m only. At larger angles of attack and control deflections, k_w becomes a nonlinear function of α and is defined using the equivalent-angle-of-attack concept.[3] The value of k_w varies from zero if no normal force results from deflection, to unity for a perfect control surface operating without any losses. The MAHAA code estimates k_w using the limited experimental data base and method described in Ref. 3.

Body Carryover Factor K_B

The increased lift on the wing for a wing–body combination arises from a changed pressure distribution on the wing due to the presence of the body. This in turn affects the pressure distribution on the body and gives rise to an incremental lift on the body. The interference factor K_B allows for this body carryover lift.

In this code, the interference factor K_B is computed using the modified SBT method of Pitts, Nielsen, and Kaattari.[6] This method computes K_B for two general cases: with an infinitely long afterbody and without afterbody. K_B for a short afterbody is obtained using the expression of Ref. 7. To take account of the losses in the carryover load at higher α, K_B is reduced according to $[K_B/K_W]_{\text{at}\,\alpha} = [K_B/K_W]_{SBT}$, where K_W at an angle of attack is obtained using the correlated database as discussed earlier. In the present method we make the approximation $[k_B/k_w] = [K_B/K_W]$, where k_B is the body carryover factor due to fin deflection. The center of pressure for the body carryover force is assumed to be at the centroid of the area projected on the body between the Mach lines from the leading and trailing edges of the fin root chord.

Body-Alone Force and Moment

The estimation of the normal force and pitching moment of the body alone[8] is carried out basically on the lines of the viscous crossflow method of Allen[9] and Perkins[10] with the modifications of Jorgensen[11] incorporated. Further improvements in the method have been achieved by introducing estimation of $C_{N\alpha}$ for the body using the charts of Ref. 12. The effect of nose bluntness on $C_{N\alpha}$ has also been included from Ref. 13.

Fin-Alone Normal-Force Coefficient C_N

The equivalent-angle-of-attack technique requires the fin-alone normal-force characteristics up to very high angles of attack (≈ 60 deg), since α_{eq} of the fins with control deflections approaches these high values. MAHAA makes use of constructed experimental data[14] for the fin-alone normal-force coefficient C_N. The experimental data are available for aspect ratios 0.5 to 4.0, taper ratios 0 to 1, Mach numbers 0.8 to 4.6, and angles of attack up to 60 deg. These data are valid for thin wings having symmetric airfoil sections with sharp leading and trailing edges. Further, the leading edge must not be swept forward, and the trailing edge sweep should be small.

Center-of-Pressure Locations

Eperimental data for the axial and lateral center-of-pressure locations (x_{cp} and y_{cp}) of the normal force for various fin planforms at angles of attack up to 60 deg have been taken from Refs. 15 and 16. The data are available for aspect ratios 0.5 to 4.0, taper ratios 0 to 1, and Mach numbers 0.6 to 4.6. These data have been correlated with the fin-alone normal-force coefficient C_N in accordance with the equivalent-angle-of-attack technique. The parameters $(x_c - x_{cp})/C$ and $(y_c - y_{cp})/s$ were chosen for correlation with C_N, where x_c and y_c are the axial and lateral centroid locations of the fin planform.

Vortex Contribution

Vortices arising from the nose of the body, the fins (canards and wings), and the afterbody travel downstream and are influenced by the local flow. The influence of the vortices on the aerodynamic characteristics could be considerable, especially at nonzero roll angles and also when two sets of fin sections are closely spaced longitudinally.

Body Vortices

The vortices shed from a body are symmetric up to a certain angle of attack depending upon the nose and body geometries, beyond which they become asymmetric. The present study assumes[2] for preliminary design purposes that the vortices are symmetrically disposed for angles of attack up to 30 deg.

The code assumes that for $\alpha < 5$ deg the body vortices are weak and have no significant effect on the aerodynamic characteristics. For $5 \le \alpha \le 10$ deg, the shed-vortex strength and position can be obtained using the method of Ref. 17. For $\alpha \ge 20$ deg, the body-vortex strengths and positions are estimated using the correlated data of Ref. 3. For $10 < \alpha < 20$ deg, a linear interpolation between the results for $\alpha = 10$ and 20 deg is adopted.[3]

Fin Vortices

The vortex field arising from the fins at angles of attack have been considered in terms of an equivalent finite number of discrete vortices. The simple procedure of Ref.18 is used to compute the strengths and positions of the fin vortices. The method requires a priori values of the fin normal force and the lateral center-of-pressure position, and these are estimated using the equivalent-angle-of-attack method.

Vortex Tracking

The vortices are tracked downstream from their initial positions using a tracking routine based on the crossflow study of SBT. In this tracking procedure, the cruciform cross section of the body is transformed into a circle using a conformal transformation, and the flowfield including the vortices is generated in the transformed plane. The flow velocities at the centers of the vortices are then computed. These flow velocities in the crossflow plane are compounded with the axial component of the freestream flow to get the total velocities at the centers of the vortices. Using these velocities, the vortex kinematic equations are written, and they have been solved numerically for different longitudinal stations along the body to get the vortex trajectories.

At nonzero roll orientation and unequal deflections of the control surfaces, the vortex strengths and positions of individual fins are different. Consequently, the vortices do not form symmetric pairs, and a modification in the imaging procedure will be required. In MAHAA this modification has been brought about by the inclusion of a third image vortex at the center of the body. The strength of this vortex depends on the degree of asymmetry in the external vortex strengths. The tracking Methodology also includes a term corresponding to the expansion of the equivalent body arising from the fins. The contribution from this will be substantial when the local fin span is large in comparison with the body radius.

Vortex-Induced Loads

The vortex-induced normal loads and moments on the fins are estimated using the reverse-flow theorem.[3] In this method, the spanwise loadings on the four fin surfaces for a unit deflection of one of the fins with $\alpha = 0$ are calculated, and a similar calculation for a linear twist distribution on one of the fins is also carried out (the former distribution is used in computing the normal force, and the latter in computing the rolling moment). The induced angle-of-attack variation along the span of the fins due to the discrete vortices is calculated using the Biot–Savart law. From these results, the normal forces and lateral positions of the centers of pressure on the fins due to the vortices are calculated using the reverse-flow theorem.

Accuracy Criteria

For any semiempirical code, it must be accepted that exact estimates will not result except for a few rare cases where the design configuration is very similar to the data base or data correlation employed in the code. Therefore, it becomes necessary to address the errors that can be allowed in their predictions for preliminary design studies.

Krieger and Williams[19] have suggested allowable errors in the Aerodynamic coefficients by relating them to the allowable errors in the final performance predictions. The user of the accuracy criteria may then select the allowable errors based on the preliminary design requirements. Reference 19 presents a typical accuracy criterion for preliminary design where the allowable errors in the side-force, normal-force, yawing-moment, pitching-moment and rolling-moment, coefficients are approximately $\pm 20\%$, and in the axial-force coefficient is approximately $\pm 10\%$. However, with more and more stringent quality requirements being put forth as a result of advances in technology, the margin for allowable errors in performance predictions will decrease considerably. It was therefore decided to reduce the allowable errors in prediction of C_N, C_Y, C_m, C_l, and C_n by half for the MAHAA code.

Code Validation

To establish the prediction capability of MAHAA, it has been extensively validated against experimental data. A total of 27 configurations, representing a wide range of missile geometries, were chosen for the validations. The predicted results were compared with the experimental data for these configurations up to high angles of attack. Some of the comparisons are illustrated in Figs. 1–9.

A typical comparison of results for a body–canard–tail configuration[20] with and without canard fins attached is shown in Fig.1. Predictions of both C_N and C_m are very close to the experimental results throughout the angle-of-attack range. A validation for the Sparrow III missile[21] at $M = 2.35$ and $\phi = 0$ is presented in Fig. 2. C_N is predicted very closely for angles of attack up to 45 deg and also with wing pitch-control deflection of 20 deg. The prediction of the pitching-moment coefficient shows fairly good agreement. Figure 3 shows a typical validation for a wing-body combination[22] at $M = 1.6$, for nonzero roll and high angles of attack. C_N and C_m are estimated well for angles of attack up to 50 deg. Figure 4 shows results for a body–tail combination[23] at a transonic Mach number of 0.8 and angles of attack up to 45 deg. The prediction of C_N is

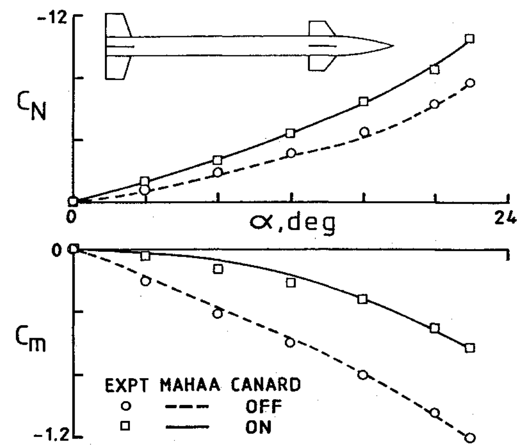

Fig. 1 Comparisons of C_N and C_m for a body-canard-tail configuration: M= 2.36, ϕ = 0.

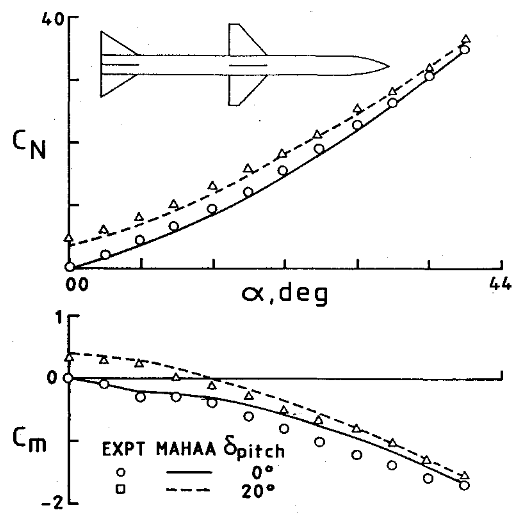

Fig. 2 Comparisons of C_N and C_m for a missile of the Sparrow III type: M = 2.35, ϕ = 0.

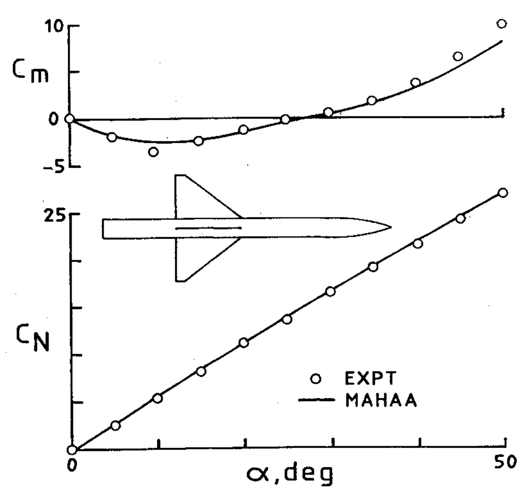

Fig. 3 Comparisons of C_N and C_m for a wing-body configuration: M = 1.6, ϕ = 22.5 deg.

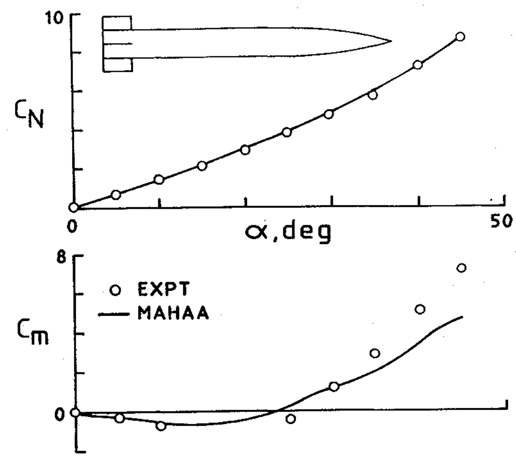

Fig. 4 Comparisons of C_N and C_m for a body-tail configuration: M = 0.8, ϕ = 0.

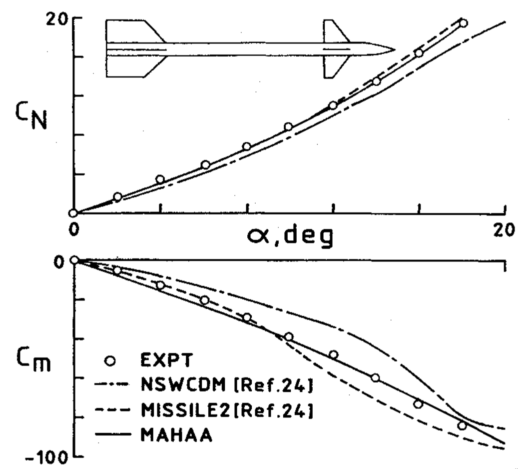

Fig. 5 Comparisons of C_N and C_m for a Sidewinder-like missile: M = 2.5, ϕ = 45 deg.

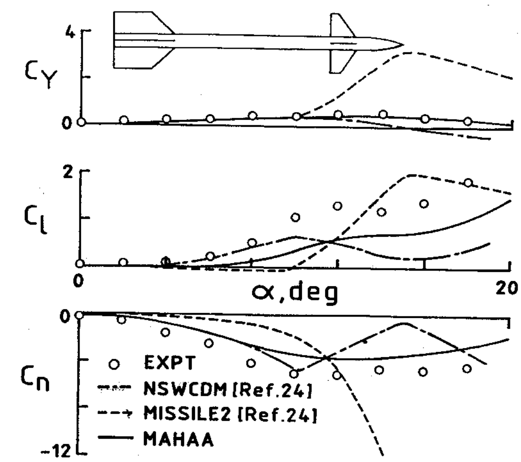

Fig. 6 Comparisons of the lateral characteristics for a Sidewinder-like missile: M = 1.75, ϕ = 26.57 deg.

accurate throughout the α range, and that of C_m is good up to about $\alpha = 35$ deg.

In Fig. 5, the predicted results for a Sidewinder-like missile are compared with those of two other prediction codes, namely NSWCDM and MISSILE2 from Ref. 24, along with the experimental data. It is observed that the coefficients C_N and C_m are predicted more accurately by the MAHAA code. The prediction of the lateral characteristics for a typical case of nonzero roll ($\phi = 26.57$ deg) is presented in Fig. 6. It is observed that C_Y is very closely predicted for the entire α range, and the predictions of C_l and C_n show trends similar to the experimental data. These predictions are also compared with those of NSWCDM and MISSILE2 codes from Ref. 24. It is clear from Fig. 6 that the present predictions of C_Y, C_l, and C_n are better than those given by the other two codes in terms of the magnitudes as well as trends. These general result was observed for other configurations for which validations were carried out in the present study. These improved predictions of the lateral characteristics seem to be the result of the emphasis laid

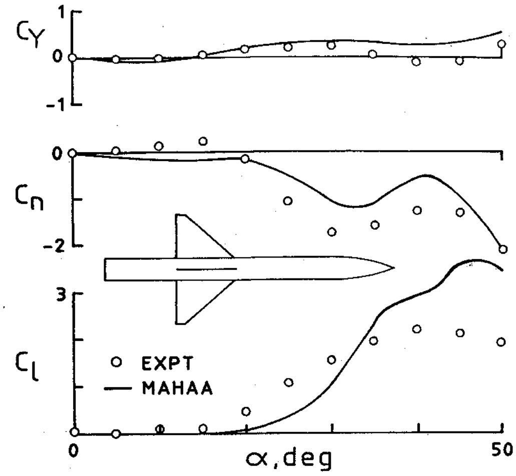

Fig. 7 Comparisons of C_Y, C_l, and C_n for a wing-body configuration: $M = 1.6$, $\phi = 22.5$ deg.

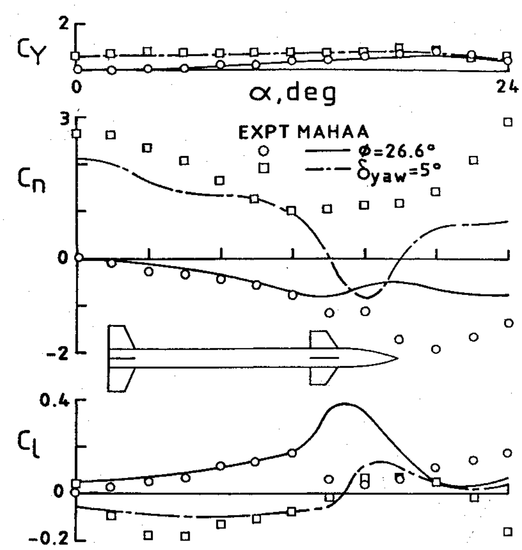

Fig. 8 Comparisons of C_Y, C_n, and C_l for a canard-controlled missile: M=2.36; at ϕ = 26.6 deg, and for δ_{yaw} = 5 deg at ϕ = 0.

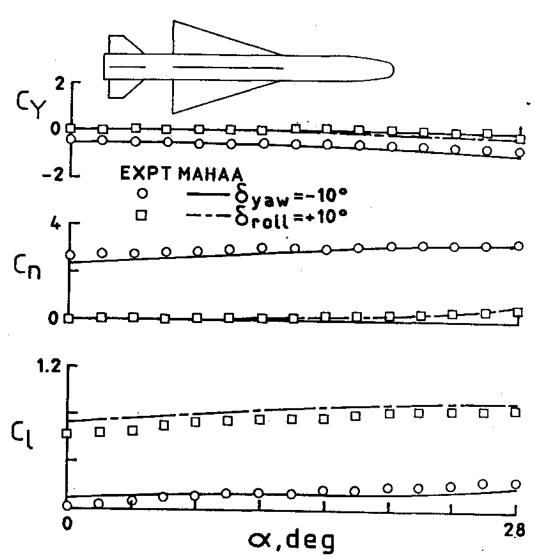

Fig. 9 Comparisons of C_Y, C_n, and C_l for a wing-body-tail configuration: M=2.86, at ϕ = 45 deg and all fins deflected.

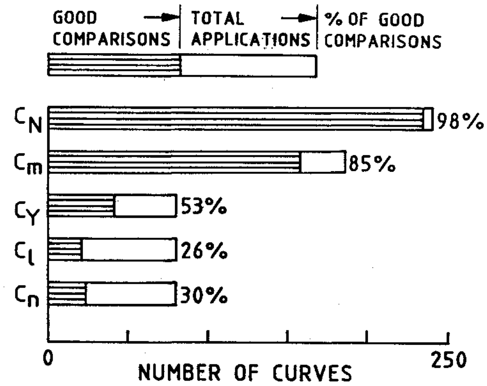

Fig. 10 Summary of prediction accuracy for the code.

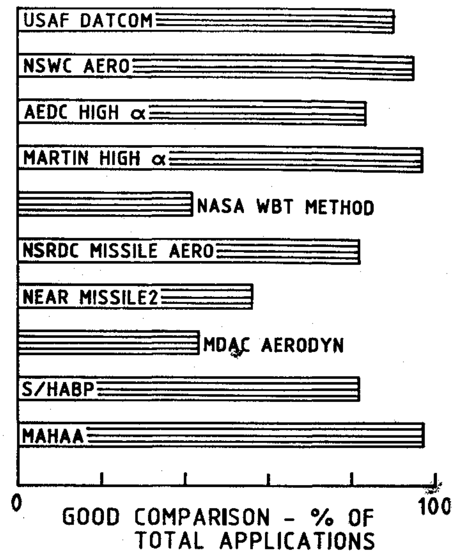

Fig. 11 Comparison of the normal-force accuracy for a conventional missile configuration.

on the vortex-tracking scheme to take account of the asymmetric situation.

The lateral characteristics of a wing–body combination of Ref. 22 up to high angles of attack and with asymmetric roll orientation is shown in Fig. 7. Here, C_Y is predicted accurately for α upto 35 deg, whereas C_l and C_n show some deviations. Figure 8 shows the prediction of the lateral characteristics of a canard-controlled missile for two cases. The first case is for a roll angle of 26.6 deg, and the second, for yaw-control deflection of 5 deg at zero roll angle. It is again observed that the prediction of C_Y is very good over the entire α range and the C_l and C_n predictions are acceptable for low angles of attack.

Figure 9 shows the effect of control deflections on the lateral and directional characteristics of a wing–body–tail configuration[25] at $\phi = 45$ deg, with all the four tail fins deflected. In the first case, the fins are deflected for yaw ($\delta_{yaw} = -10$ deg), and in the second, for roll ($\delta_{roll} = 10$ deg). The estimates of C_Y, C_l, and C_n are good for the entire α range. This validation exemplifies an important feature of this code, viz., the lateral and directional characteristics of the configuration are estimated better for missile configurations at symmetric roll orientations ($\phi = 0$ or 45 deg) with control deflections than for asymmetric cases.

Comparison with Other Codes

A comparative study of eight semiempirical codes and one panel code is available in Ref. 26, where their relative capabilities have been assessed. The results are presented in terms of the good predictions (which conform to the accuracy criteria prescribed earlier) expressed as a precentage of the total number of predictions made. The exercise was followed for MAHAA and is included for comparison with these nine codes.

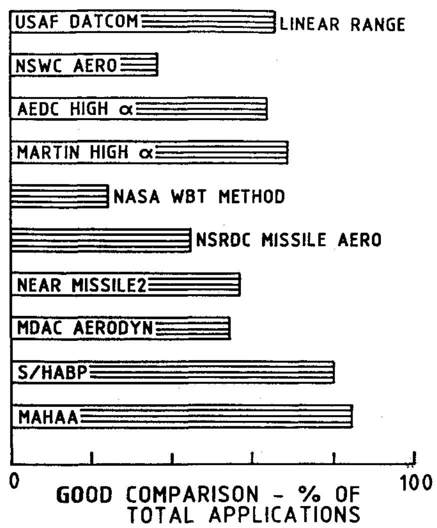

Fig. 12 Comparison of the pitching-moment accuracy for conventional missile configuration.

A summary of the prediction accuracy for MAHAA is given in Fig. 10 for the five aerodynamic coefficients. A total of 27 configurations have been used in this study.[2] It is observed that 98% of the predictions for C_N and 85% of the predictions for C_m are good and within the prescribed accuracy requirements. For C_Y, C_l, and C_n the percentage of good comparisons is drastically lower: 53, 26, and 30%, respectively. As discussed previously, predictions of C_l and C_n are not so good at higher angles of attack for asymmetric roll orientations; however they show good qualitative trends with respect to the experimental results.

The prediction accuracy of MAHAA for normal-force and pitching-moment coefficients is compared with that of nine other codes in Figs. 11 and 12. The majority of the codes have 80% or higher good comparisons for normal force, and for pitching moment it is in the 40 to 60% range. The MAHAA code shows 98% and 85% good comparisons for C_N and C_m respectively, which is a considerable improvement over the other codes. Keeping in view the improvements that may have been made in the nine codes subsequent to their publication, it can still be concluded from these comparisons that MAHAA is a state-of-the-art missile aeroprediction code.

Conclusions

The equivalent-angle-of-attack methodology is a powerful technique for predicting the aerodynamic characteristics of missile configurations in the nonlinear ranges of angle of attack and Mach number with nonzero roll angles and control deflections. The MAHAA code has exploited the potential of the equivalent-angle-of-attack concept for a more accurate prediction capability by considering vast correlated experimental databases of wing-alone characteristics, centers of pressure, and wing-body interference. This has resulted in very close predictions of the normal-force and pitching-moment characteristics up to very high angles of attack and with control deflections. A comparative study with other missile aeroprediction codes has clearly brought out the improved capability of the MAHAA code. Also, the correlated-data approach used in MAHAA has resulted in substantial reduction in the bulk of the data inputs.

The prediction capability of MAHAA for the lateral characteristics is found to be good for a large number of validations carried out, and the qualitative trends of these characteristics have been reproduced. The vortex-tracking scheme appropriate to asymmetries associated with large roll angles and arbitrary control deflections is mainly responsible for this improvement. The agreement for the side-force coefficient C_Y is better than for rolling- and yawing-moment coefficients. This, together with the fact that the qualitative trends of C_l and C_n are reproducible in a large number of cases, suggests that it is possible to improve the predictions of these characteristics by using better inputs for the data on the lateral center of pressure.

Acknowledgments

The work reported herein was performed at the National Aeronautical Laboratory (NAL), India, under the sponsorship of the Defence Research and Development Laboratory (DRDL), India. The authors acknowledge the help received from S. N. Seshadri, NAL, and S. Panneerselvam, DRDL, through valuable discussions and suggestions.

References

[1]Hemsch, M. J., and Nielsen, J. N., "The Equivalent Angle-of-Attack Concept for Engineering Analysis," *Tactical Missile Aerodynamics*, edited by M. J. Hemsch and J. N. Nielsen, Progress in Astronautics and Aeronautics, Vol. 104, AIAA, New York, 1986, Chap. XI, pp. 482–518.

[2]Venugopal, S., and Krishnamurthy, M., "A high Angle of Attack Aerodynamic Prediction Code for Cruciform Missile Configurations," National Aeronautical Laboratory, India, PD EA, 1204, May 1992.

[3]Nielsen, J. N., Hemsch, M. J., and Smith, C. A., "A Preliminary Method for Calculating the Aerodynamic Characteristics of Cruciform Missiles to High Angles of Attack Including Effects of Roll Angle and Control Surface Deflections," Office of Naval Research, Rept. ONR CR215-226-4F, Arlington, VA, Nov. 1977.

[4]Krishnamurthy, M., and Venugopal, S., "A Correlation Study of the Wing–Body Interference Factor for High Angles of Attack," *Journal of the Aeronautical Society of India*, Vol. 43, No. 2, 1991, pp. 93–99.

[5]Nielsen, J. N., *Missile Aerodynamics*, McGraw–Hill, New York, 1960, pp. 114–143.

[6]Pitts, W. C., Nielsen, J. N., and Kaattari, G. E., "Lift and Center of Pressure of Wing–Body–Tail Combinations at Subsonic, Transonic and Supersonic Speeds," NACA TR 1307, 1957.

[7]*Method for Estimating the Normal Force Coefficient of Delta Wing–Body Combinations at Supersonic Speeds at Incidences up to 25 Degrees*, Vol. 4, Item No. 68022, Engineering Science Data Unit, London, 1970.

[8]Ramesh, K., and Krishnamurthy, M., "A Computer Code to Estimate the Normal Force and Pitching Moment Characteristics of Axisymmetric Bodies upto High Angles of Attack," National Aeronautical Laboratory, India, PD EA 9002, Feb. 1990.

[9]Allen, H. J., "Estimation of the Forces and Moments Acting on Inclined Bodies of Revolution of High Fineness Ratio," NACA RM-A9I26, Nov. 1949.

[10]Perkins, W. E., and Jorgensen, L. H., "Comparison of Experimental and Theoretical Normal Force Distribution (Including Reynolds Number Effects) on an Ogive-Cylinder Body at Mach Number 1.98," NACA TN 3716, May 1956.

[11]Jorgensen, L. H., "Prediction of Static Aerodynamic Characteristics for Slender Bodies Alone and with Lifting Surfaces to Very High Angles of Attack," NASA TR R-474, Sept. 1977.

[12]*Normal-Force Curve Slope and Center of Pressure Position at Zero Angle of Attack for Tangent Ogive Cylinder and Cone Cylinder Combinations at Supersonic Speeds*, Vol. 3, Item No. 86029, Engineering Science Data Unit, London, 1986.

[13]Ingram, C. W., Ball, K. O. W., Dinkeloo, C., and Shida, D., "Preliminary Design Aerodynamic Prediction Methodology for Missiles with Nose Bluntness," Air Force Flight Dynamics Lab., TR 78-117, Sept. 1978.

[14]Venugopal, S., and Krishnamurthy, M., "A Computer Code Based on Experimental Data Base to Estimate the Fin Alone Normal Force Characteristics upto High Angles of Attack," *Journal of the Aeronautical Society of India*, Vol. 42, No. 4, 1990, pp. 293–298.

[15]Nielsen, J. N., and Goodwin, F. K., "Preliminary Method for Estimating Hinge Moments of All-Movable Controls," Nielsen Engineering and Research, Inc., TR 268, Mountain View, CA, March 1982.

[16]Briggs, M. M., Reed, R. E., and Nielsen, J. N., "Wing-Alone Aerodynamic Characteristics to High Angles of Attack at Subsonic and Transonic Speeds," Nielsen Engineering and Research, Inc., TR 269, Mountain View, CA, Nov. 1982.

[17]Mendenhall, M. R., and Nielsen, J. N., "Effect of Symmetrical Vortex Shedding on the Longitudinal Aerodynamic Characteristics of Wing–Body–Tail Combinations," NASA CR 2473, Jan. 1975.

[18]Hemsch, M. J., Smith, C. A., Nielsen, J. N., and Perkins, S. C., Jr., "Calculation of Component Forces and Moments of Arbitrarily Banked Cruciform Missiles with Control Deflections," Office of Naval Research, Rept. ONR CR215-226-3, Arlington, VA, Nov. 1976.

[19]Krieger, R. J., and Williams, J. E., "Accuracy Criteria for Evaluating Supersonic Missile Aerodynamic Coefficient Predictions," *Journal of Spacecraft and Rockets*, Vol. 20, No. 4, 1983, pp. 323–330.

[20]Blair, A. B., Jr., "Wind Tunnel Investigation at Supersonic Speeds of a Canard-Controlled Missile with Fixed and Free Rolling Tail Fins," NASA TP 1316, Sept. 1978.

[21]Monta, W. J., "Supersonic Aerodynamic Characteristics of a Sparrow III Type Missile Model with Wing Control and Comparison with Existing Tail-Control Results," NASA TP 1078, Nov. 1977.

[22]Stallings, R. L., "Effect of Reynolds Number on Stability Characteristics of a Cruciform Wing–Body at Supersonic Speeds," NASA TP 1683, July 1980.

[23]Derrick, J. N., Spring, D. J., and Winn, G. C., "Aerodynamic Characteristics of a Series of Bodies With and Without Tails at Mach numbers from 0.8 to 3.0 and Angles of Attack from 0 to 45 Degrees," U.S. Army Missile Command, Rept. TR-RD-7T-3, Redstone Arsenal, AL, July 1976.

[24]Blair, A. B., Jr., Allen, J. M., and Hernandez, G., "Effect of Tail Fin Span on Stability and Control Characteristics of a Canard Controlled Missile at Supersonic Mach Numbers," NASA TP 2157, June 1983.

[25]Corlette, W. A., "Supersonic Stability and Control Characteristics of a Cruciform Missile Model with Delta Wings and Aft Tail Fin Controls," NASA TM 80171, Dec. 1979.

[26]Baker, W. B., Jr., "Use of Semiempirical Aerodynamic Methods for Preliminary Design, (Proceedings-Missile Aerodynamics)" *NEAR Conference on Missile Aerodynamics* (Monterey, CA), 1988, pp. 6-1–6-28.

J. M. Allen
Associate Editor

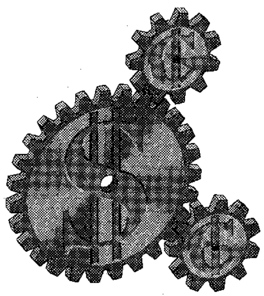

INTRODUCTION AND METHODOLOGY OF SPACE COST ENGINEERING

April 26-28, 1995 Washington, DC

This seminar will provide the tools and knowledge for space professionals to face the next decade of cost reductions as well as increasing performance demands from the political and technological communities.

HOW YOU WILL BENEFIT FROM THIS COURSE

Learn how cost engineering can contain the cost of a project.
Discover why cost engineering has become an essential tool.
Learn better ways to assess the validity and limits to cost estimates.
Learn how to define and develop a costing methodology.
Find the best way to evaluate cost related project risks.

INSTRUCTOR

Richard Boudreault, Aerospace Technologies Inc.

For more detailed information call or FAX Johnnie White
Phone: 202/646-7447
FAX: 202/646-7508

AIAA
American Institute of Aeronautics and Astronautics